ACTA CHEMICA SCANDINAVICA 26 (1972) 3101–3113

Magnetic Structure and Properties of FeAs

KARI SELTE,[a] ARNE KJEKSHUS[a] and ARNE F. ANDRESEN[b]

[a]*Kjemisk Institutt, Universitetet i Oslo, Blindern, Oslo 3, Norway and* [b]*Institutt for Atomenergi, Kjeller, Norway*

Iron mono-arsenide has been investigated by X-ray and neutron diffraction, magnetic susceptibility, differential thermal analyses, and diffuse reflectance measurements. The crystal structure remains essentially of the MnP type between 12 and ~ 1300 K. Below a Néel temperature of 77 ± 1 K a helimagnetic structure is adopted, with a spiral propagation vector of $0.375 \times 2\pi\mathbf{c}^*$ and a moment of 0.5 ± 0.1 μ_B per Fe atom at 12 K. The relationship between the magnetic structures of FeAs and other compounds with MnP type atomic arrangement is discussed. The magnetic susceptibility of FeAs (determined from 4.2 to ~ 1000 K) satisfies the Curie-Weiss Law between ~ 300 and ~ 650 K with $\theta = -1400 \pm 200$ K and $\mu_P = 3.1 \pm 0.4$ μ_B per Fe atom. Below ~ 300 K and above ~ 650 K there are deviations from the Curie-Weiss Law.

Until some five years ago, studies on compounds with the MnP type crystal structure dealt mainly with phase analytical and structural problems (*cf.*, *e.g.*, Ref. 1). More recently, however, there has occurred a shift in emphasis towards the magnetic properties. The alteration in viewpoint is a result of the interesting spiral structures which have been found successively for MnP,[2–5] CrAs,[6–8] and FeP.[9] (A similar feature is also predicted for MnAs [10] at high pressures, whereas no cooperative magnetic phenomenon is found [11] at normal pressure.) Although certain indications of this behaviour could be found in the magnetic susceptibility data for these compounds, the interesting details were first observed after a systematic application of the neutron diffraction technique.

The fact that all known examples of cooperative magnetism for compounds with the MnP type structure belong to the helimagnetic class (except the interval $50 < T < 291.5$ K for the prototype compound itself, where ferromagnetism prevails [12,13]) suggests very strongly that this behaviour is a consequence of their atomic arrangement, *viz.* in particular the geometry of the metal atom sublattice. For this reason, FeAs was regarded as a highly suitable candidate for a low temperature neutron diffraction study. With the exception of a recent investigation [14] of the crystal structure of FeAs, information about the physical properties is almost completely lacking for this compound.

EXPERIMENTAL

The samples were prepared from 99.99+ % Fe (Johnson, Matthey & Co., Ltd; turnings from rods) and 99.999+ % As (Fluka AG) by heating equiatomic quantities of the components in evacuated and sealed silica tubes. A sample of approximately 100 g was heated for 10 days at 850°C. After careful grinding, the sample was reheated at 850°C for another 10 days and cooled to room temperature over 3 days. This sample was used for all the different measurements described below. Crystals of FeAs were easily grown by an iodine transport reaction. These were used for duplicate magnetic property measurements.

Powder neutron diffraction data were collected at various temperatures between 12 and 293 K using cylindrical sample holders of vanadium. Neutrons of wavelength 1.863 ± 0.001 Å were obtained from the JEEP II reactor. The nuclear scattering lengths ($b_{Fe} = 0.95 \times 10^{-12}$ cm, $b_{As} = 0.64 \times 10^{-12}$ cm) were taken from the table published by *The Neutron Diffraction Commission* [15] and the magnetic form factor for Fe^{3+} from Watson and Freeman.[16] The least squares profile refinement programme written by Rietveld [17] was applied in the final fitting of the variable parameters to the observed intensity data. The following parameters were refined: the scale factor, the counter zero point, three profile parameters, the unit cell dimensions, the positional parameters, and isotropic temperature factors for both kind of atoms. Calculated standard deviations are appended in brackets after the corresponding parameter values.

High temperature X-ray powder photographs were obtained in a 190 mm diameter Unicam camera with the samples sealed in thin-walled quartz capillaries using Fe$K\alpha$ radiation. The temperature of the furnace surrounding the specimen was kept constant to within ± 5°C during the exposures. The Pt/Pt-Rh thermocouples of the furnace were calibrated with a standard couple located at the position of the specimen. Lattice dimensions were determined from the high-angle reflections, using the Nelson-Riley [18] type extrapolation.

The magnetic susceptibilities of FeAs samples were measured between 80 and 1000 K by the Faraday method (maximum field ~ 8kØ) using 30 – 50 mg samples, and from 4.2 K to room temperature at field strengths up to 15 kØ in a Princeton Applied Research Model FM-1 vibrating sample magnetometer. Samples of ~ 300 mg were utilized in the latter measurements.

A DTA analysis was accomplished with a Mettler Recording Vacuum Thermoanalyzer using a 200 mg sample in a sealed silica capsule. The heating rate was 4°C/min and Fe-powder (200 mg) was used as reference material. The maximum temperature attained was 900 K.

Diffuse reflectance measurements were made in the range 2400 to 20 000 Å using a Cary 14 dual-beam spectrophotometer fitted with a diffuse reflectance accessory. $MgCO_3$ was used as a standard, and the integrating sphere was coated with MgO.

RESULTS

(i) *Chemical crystal structure.* FeAs has no appreciable range of homogeneity and its composition is unequivocally confirmed to satisfy the stoichiometric formula.[14] On the basis of three-dimensional single crystal X-ray data the structure of FeAs is found to be essentially of the MnP type.[14] However, the deduced space group ($Pna2_1$) lacks a mirror plane compared with that ($Pnma$) assumed for the structure of MnP. The most notable consequence of this deficiency is the complete non-equivalence of the interatomic Fe – As distances. On the other hand, this amounts to only a minor part of the total irregularity of the atomic arrangements around Fe and As.

These single crystal results may be compared with those obtained from powder samples by means of the neutron diffraction technique. The small number of reflections accessible by the latter method, imposes the constraint of isotropic temperature factors in the models subject to refinement. Attempted

Table 1. Unit cell dimensions and positional parameters for FeAs according to space group *Pnma*. (X-Ray diffraction results are quoted from Ref. 14.)

Technique		Neutron diff.	Neutron diff.	Neutron diff.	Neutron diff.	X-Ray diff.
T (K)		12	78	100	293	293
a (Å)		5.454(1)	5.454(1)	5.454(2)	5.437(2)	5.4420(7)
b (Å)		3.325(1)	3.329(1)	3.330(1)	3.370(1)	3.3727(6)
c (Å)		6.029(1)	6.027(1)	6.027(2)	6.023(2)	6.0278(7)
Fe in 4(c)	x	0.0058(8)	0.0026(6)	0.0047(6)	0.0063(7)	0.0027(5)
	z	0.1993(5)	0.1986(4)	0.1988(4)	0.1975(4)	0.1994(5)
As in 4(c)	x	0.2005(8)	0.2018(7)	0.2021(6)	0.2018(7)	0.1993(4)
	z	0.5741(9)	0.5771(8)	0.5768(8)	0.5789(6)	0.5774(4)

refinements of the room temperature data in terms of a model based on space group $Pna2_1$ gave no convergence in the calculations. This negative result, which clearly can be attributed to the paucity of relevant observations, is in complete accordance with previous experience.[7,19,20] With the y-parameters of Fe and As fixed at 1/4 in accordance with the requirements of space group *Pnma*, the profile refinements rapidly converged to the parameter values listed in Table 1. The room temperature values of x and z derived in this

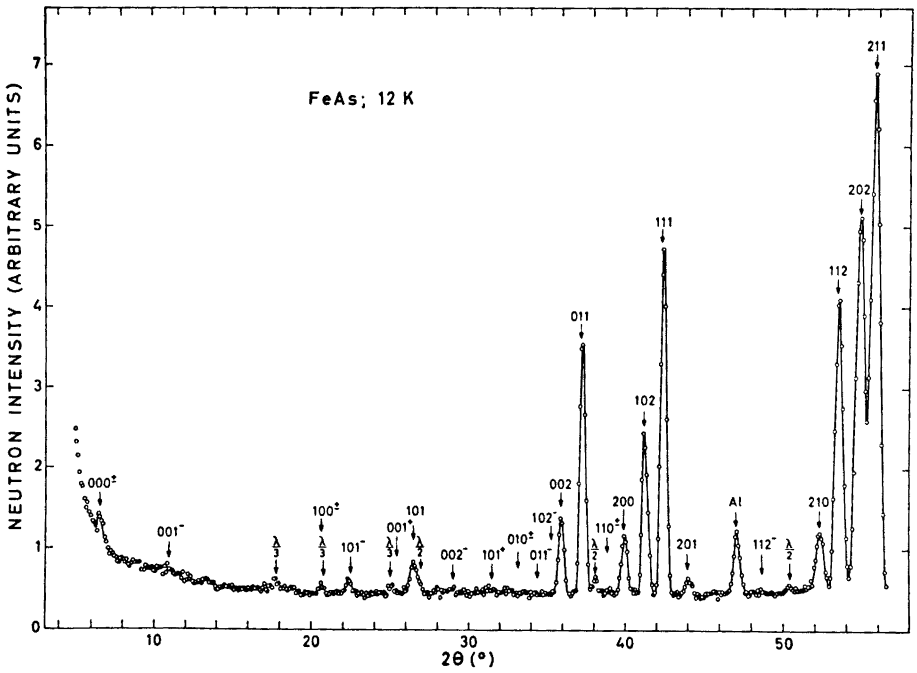

Fig. 1. Neutron powder diffraction diagram of FeAs at 12 K.

manner are in reasonable agreement with those quoted from the single crystal X-ray study.[14] Hence, although the use of the powder diffraction method does not allow an examination of those details of the structure which are governed by the absence of the mirror plane, it provides an adequate overall description of the structure, and good average values for the interatomic distances.

The results of powder X-ray and neutron diffraction measurements between 12 and 1300 K show that the structure remains virtually unchanged within these limits. (The lower limit is determined by a temporary deficiency in the cryostat system, and the upper by the melting point of FeAs.) The profile refinement technique (subject to the above constraints) was applied to the neutron diffraction data collected at 12 (Fig. 1), 78, and 100 K, including only the nuclear reflections. The refinement processes were continued until negligible shifts were obtained for all variables. The resulting values for the unit cell dimensions and positional parameters are included in Table 1.

The crystallographic changes which have occurred between 293 and 12 K can be attributed to a combination of thermal contraction and magnetostriction (see section ii). Important interatomic distances at the two temperatures, listed in Table 2, show that the variations in unit cell dimensions are com-

Table 2. Shortest interatomic distances (in Å) in the crystal structure of FeAs, based on data from Table 1. (X-Ray diffraction results for 293 K.)

Type	12 K	293 K
Fe – As(1)	2.343(7)	2.347(4)
Fe – As(2)	2.428(5)	2.421(3)
Fe – As(2)	2.429(5)	2.452(3)
Fe – As(1)	2.497(7)	2.517(4)
Fe – As(average)	2.426	2.435
Fe – Fe(2) [a]	2.795(2)	2.789(2)
Fe – Fe(2) [b]	2.923(5)	2.937(5)
Fe – Fe(2) [c]	3.325(1)	3.373(1)
As – As(2)	2.889(5)	2.902(3)

[a] Distance between Fe atoms 1 and 2 (3 and 4). [b] Distance between Fe atoms 2 and 3 (4 and 1). [c] Distances along the *b* axis.

pensated by shifts in the atomic positions, so that the average bond lengths remain virtually unchanged. Analogous behaviour has been observed for CrAs.[7]

(ii) *Thermal expansion.* Anomalies found in the initial measurements of the temperature dependence of the magnetic susceptibility (see section iii) were the immediate incentive for performing a high temperature X-ray examination of FeAs. There is no indication of changes in lattice symmetry above room temperature, and the essentially invariable relative intensities of the reflections confirm that the positional parameters are approximately independent of temperature up to ~1300 K. (The present value of 1070 ± 20°C for the melt-

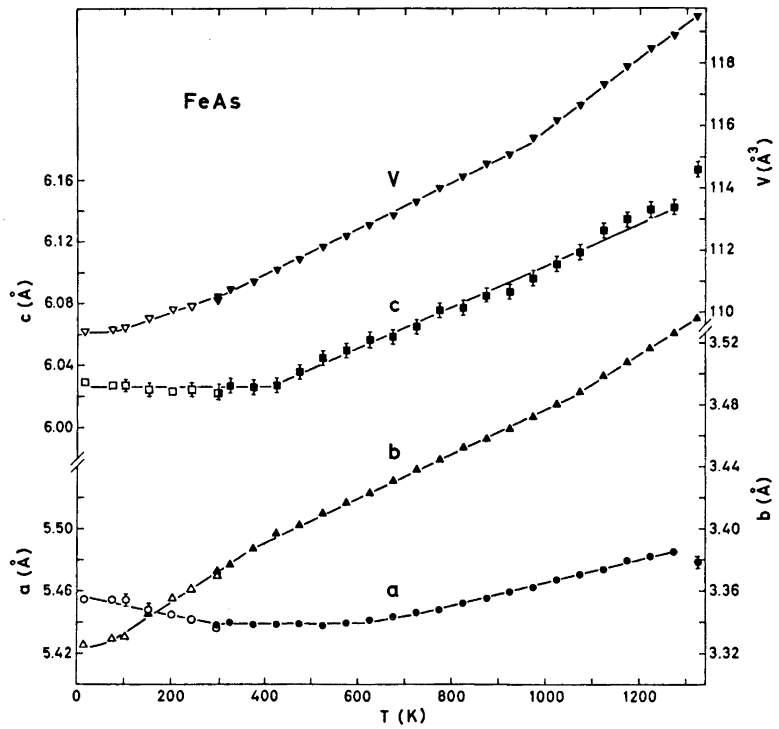

Fig. 2. Temperature dependence of unit cell dimensions of FeAs. Open and filled symbols represent neutron and X-ray diffraction data, respectively. Vertical bars show estimated error limits when these exceed the size of the symbols.

ing point of FeAs is slightly higher than that (1030°C) given by Hansen.[21] Only insignificant differences occur in the temperature dependence of the profiles of the reflections, implying that the crystalline perfection of the sample remains virtually unchanged $< \sim 1300$ K.

The combined neutron and X-ray diffraction results for unit cell dimensions, in the interval 12 – 1325 K, are shown as function of temperature in Fig. 2. The results from the two methods are seen to be in agreement at room temperature. The X-ray data above room temperature form smooth curves which are reproducible for conditions of both increasing and decreasing temperature. The data of Heyding and Calvert [22] over this temperature range are in poor agreement with those of Fig. 2. (The results of these authors are rather sparse and show considerable scatter.)

Starting from the lowest temperatures, a contracts slightly up to ~ 300 K, from which temperature a plateau extends to ~ 600 K. Some expansion in a is evident at higher temperatures. With increasing temperature, the rate of the expansion in b remains approximately constant for $T > 12$ K, the rate being substantially greater than for a. In the case of c a constancy of value at the lower temperatures is interrupted by a discontinuity in slope at ~ 400 K.

The behaviour of a, b, and c at the lowest temperatures in Fig. 2 show that magnetostriction, consequent upon the magnetic ordering below the Néel temperature of ~ 77 K (see section iv), is of minor importance for the variation in the unit cell dimensions. As seen from Fig. 2 there appears to be no first order transition associated with the magnetic ordering in FeAs as opposed to the situation in CrAs.[7,8] Although the expansion curves above room temperature show one or more discontinuities of slope there is no correlation between these and the anomalies noted in the initial magnetic susceptibility data above ~ 600 K. The origin of the discontinuities in slope of the individual expansion curves is unknown, and their nature merits further attention.

The value of the expansion coefficient, $(a_T - a_{T'})/a_{293}(T - T')$, in the a direction is -12×10^{-6} and 14×10^{-6} K^{-1} for the linear non-horizontal sections (12 – 300 and 775 – 1275 K) of the curve. Similar expressions for b, c, and V yield the values: 59×10^{-6} K^{-1} (100 – 375 K), 42×10^{-6} K^{-1} (375 – 1075 K) and 58×10^{-6} K^{-1} (1075 – 1325 K) for b, 23×10^{-6} K^{-1} (425 – 1275 K) for c, and 48×10^{-6} K^{-1} (100 – 300 K), 68×10^{-6} K^{-1} (300 – 975 K) and 104×10^{-6} K^{-1} (975 – 1325 K) for V.

(iii) *Magnetic susceptibility.* The magnetic susceptibility of a number of different stoichiometric FeAs samples was measured over the temperature range 4.2 – ~ 1000 K.

Although samples heated to $< \sim 650$ K show reproducible characteristics, a notable feature of the results obtained with higher maximum temperatures was a degree of irreproducibility between different samples. Key aspects of the thermomagnetic curves remain unaltered, however. The conformity concerns a similarity in shape of the various $\chi^{-1}(T)$ curves below ~ 650 K. In all cases, a broad minimum at ~ 250 K is followed by a linear section which extends from ~ 300 to ~ 650 K. Individual $\chi^{-1}(T)$ curves are, however, displaced by up to ~ 50 % parallel to the χ^{-1} axis, the actual level depending on the previous history of the sample. The latter factor has, on the other hand, an even greater influence on the behaviour of the $\chi^{-1}(T)$ curve above ~ 650 K. All samples which were exposed to the atmosphere show an anomaly above ~ 650 K in that their $\chi^{-1}(T)$ curves pass through a secondary minimum at ~ 700 K during the first heating. The magnitude of the minimum appears to be governed by the length of time during which the sample is in contact with oxygen, as well as particle size and other surface properties. This minimum, which is found on the first heating, is absent on cooling, where instead a discontinuity in slope occurs at ~ 800 K.

The high temperature X-ray data show, as discussed in section ii, that there is no lattice anomaly which can be correlated with the anomalous behaviour of $\chi^{-1}(T)$ above ~ 650 K. In addition, Guinier photographs of samples quenched from various points of the temperature cycle are identical. As a further means of investigation, DTA curves were obtained for typical samples (which had been in contact with oxygen). During the first heating a detectable endothermic effect was found in the vicinity of 775 K. This anomaly was absent on cooling and in further temperature cycles. At first sight the anomalies in the $\chi^{-1}(T)$ and DTA curves appear to depend on possible surface phenomena such as oxidation.

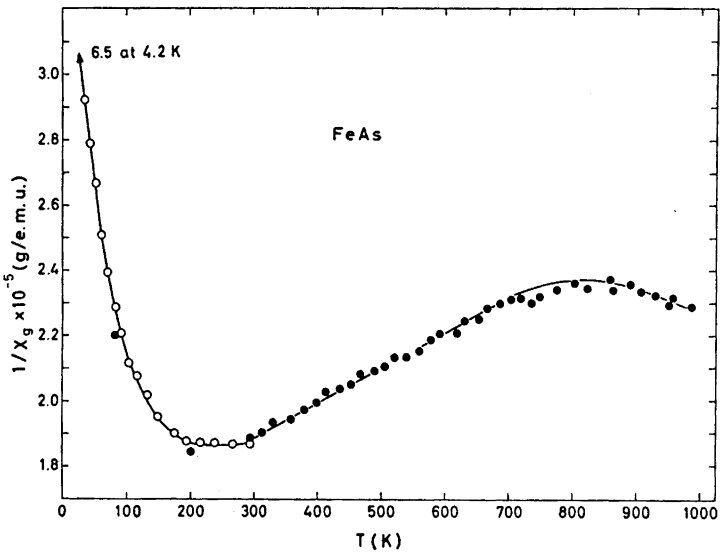

Fig. 3. Inverse magnetic susceptibility *versus* temperature for FeAs. Open circles denote values obtained with the magnetometer, filled circles with the Faraday balance.

With these properties in mind, it was found possible to prepare samples lacking the high temperature anomaly in $\chi^{-1}(T)$, and giving reproducible characteristic for conditions of both increasing and decreasing temperature. The magnetic susceptibility of such a sample between 4.2 and ~1000 K is shown in Fig. 3. Field strength dependence was not observed and the experimental points represent mean values obtained at several different field strengths. The data are uncorrected for induced diamagnetism since reliable corrections are not easily estimated.

From the linear section of the $\chi^{-1}(T)$ curve in Fig. 3, following the Curie-Weiss Law, $\chi^{-1}=C^{-1}(T-\theta)$, a θ value of -1400 ± 200 K is found. The slope (C^{-1}) which is common to *all* samples (within the experimental error) gives $\mu_P=\sqrt{8C_{mol}}=3.1\pm0.4$ μ_B per Fe atom. The equivalent spin quantum number according to the "spin only" approximation ($\mu=g\sqrt{S(S+1)}$ with $g=2$) is $S=1.1\pm0.2$. Below ~300 K $\chi^{-1}(T)$ shows a positive deviation from the Curie-Weiss Law relationship.

The diffuse reflectance of FeAs decreases uniformly from 2400 to 20 000 Å, with no observed absorption edge or other anomalies. This implies that FeAs belongs to the metallic class of conductors.

(iv) *Magnetic structure.* The occurrence of magnetic ordering in FeAs is established by the presence of additional reflections in the neutron diffraction diagram at 12 K (*cf.* Fig. 1). There is a clear relationship between this diagram and those obtained for CrAs below the Néel temperature,[6–8] suggesting the existence of a double spiral arrangement. The positions of the satellite

reflections define the propagation vector as $0.375 \times 2\pi\mathbf{c}^*$ (*i.e.* with spiral axis along *c*). Further parameters specifying the spirals are obtained from the characteristic absences governing the satellite reflections and the intensities of those present (*cf.* Refs. 2, 3, 6 – 9).

Employing the same labelling system of the four equivalent metal positions in the chemical unit cell as was introduced for CrAs,[7] the Fe atoms are referred to as follows:

$$(1)\ x,\tfrac{1}{4},z;\quad (2)\ \tfrac{1}{2}+x,\tfrac{1}{4},\tfrac{1}{2}-z;\quad (3)\ \tfrac{1}{2}-x,\tfrac{3}{4},\tfrac{1}{2}+z;\quad (4)\ \bar{x},\tfrac{3}{4},\bar{z},$$

the values of x and z being given in Table 1. As has already been established for MnP, CrAs, and FeP, the magnetic moments are assumed to be at right angles to the spiral axis in the absence of a magnetic field.[2,3,6–9] The two unknown parameters to be determined from the intensities of the satellites are the phase angle ϕ between the independent spirals through atoms 1 and 2, and the value of the magnetic moment $\mu(=2S_{Fe})$, *viz.* assuming equal moments on atoms 1 and 2. A step-wise refinement procedure similar to that employed for CrAs [7] yielded $\mu = 0.5 \pm 0.1\ \mu_B$ and $\phi = 140 \pm 10°$ for FeAs at 12 K. The higher error limits result from reduced intensity levels of the satellites in the present case. The calculated and observed intensities of the satellites are compared in Table 3.

Table 3. Observed (at 12 K) and calculated intensities of satellite reflections for FeAs.

h k l	I_o	I_c	*h k l*	I_o	I_c
$000^{\pm}$	356	364	101^{+}	105	104
001^{-}	–	0	$010^{\pm}$	–	0
$100^{\pm}$	–	0	011^{-}	–	0
101^{-}	298	289	102^{-}	–	0
001^{+}	–	0	$110^{\pm}$	52	108
002^{-}	78	10	112^{-}	120	76

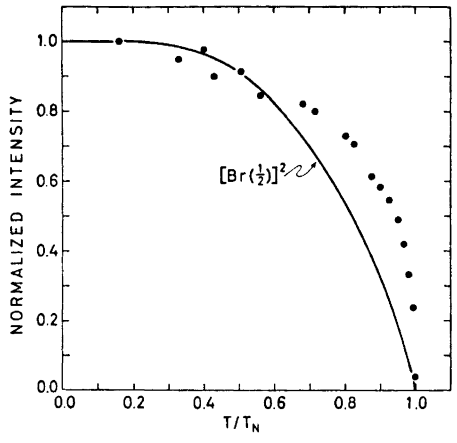

Fig. 4. Temperature dependence of the normalized intensity of the 101^{-} satellite for FeAs.

The integrated intensity of the $10\bar{1}$ satellite was used to determine the Néel temperature, $T_N = 77 \pm 1$ K. In contrast with findings for CrAs,[7,8] no hysteresis was found in the temperature dependence of the satellite intensities for FeAs. The normalized integrated intensity of $10\bar{1}$ *versus* reduced temperature is presented in Fig. 4, where it is seen that the experimental points do not follow a Brillouin type function. This appears to be a general phenomenon for compounds with helimagnetic structures.

Apart from the effective reduction of μ for T approaching T_N, the parameters specifying the spirals (*i.e.* period and mutual phase shift) appear, to the attainable accuracy, insensitive to temperature variations.

DISCUSSION

The MnP type crystal structure is found extensively among the monopnictides of the 3*d* transition metals. A notable feature of the nine phosphides and arsenides in this class of compounds (*viz.* VAs, CrP, CrAs, MnP, MnAs, FeP, FeAs, CoP, and CoAs) is the high degree of constancy observed in the axial proportions of the unit cells. In addition, the positional parameters of the metal atoms vary little, whereas slightly larger variations are found in the positions of the non-metal atoms.[7,8,14,20,23–25]

Typical of the magnetic structures of CrAs, MnP, FeP, and FeAs are double helical spin arrangements with spiral axes parallel to the common *c* axis, as shown in Fig. 5. The large variation in the moment orientations is reflected in the wide variety of spiral parameters listed in Table 4. From the latter data it may be seen that there is an empiric correlation between the atomic number of the metal and magnetic moment, phase difference, and Néel temperature in that μ and T_N decrease, while $\phi_{1,2}$ increases monotonically from Cr, through Mn to Fe. The consequent correlation between μ and $\phi_{1,2}$ is seen in Fig. 6. On the other hand, the spiral period appears to depend mainly on structural details peculiar to the combinations of metal and non-metal atoms (*cf.* Table 4).

The correlations described above are compatible with the experimentally found absence of cooperative magnetism in CoAs, [20] which may also be predicted to be the case in CoP. Similarly, CrP and in particular, VAs may be

Table 4. Data for the helimagnetic states of CrAs, MnP, FeP, and FeAs.

Compound	T (K)	μ (μ_B)	$1/\tau$ (*c* lengths)	$\phi_{1,2}$(°)	T_N(K)	Ref.
CrAs	96	2.0	2.83	−89	~280	6
CrAs	80	1.70 ± 0.05	2.83	-133 ± 1	261 − 272	7
CrAs	4	1.67 ± 0.06	2.67	-126 ± 5	238 − 248	8
CrAs	198	1.52 ± 0.04	2.86	-117 ± 4	238 − 248	8
MnP	4	1.3 ± 0.1	8.6	16	(> 50)	2
MnP	4	$1.5_9 \pm 0.1$	8.2_0	16.1 ± 0.2	(> 50)	3
FeP	4	0.41 av.	5.0	168.8	125 ± 1	9
FeAs	12	0.5 ± 0.1	2.67	140 ± 10	77 ± 1	

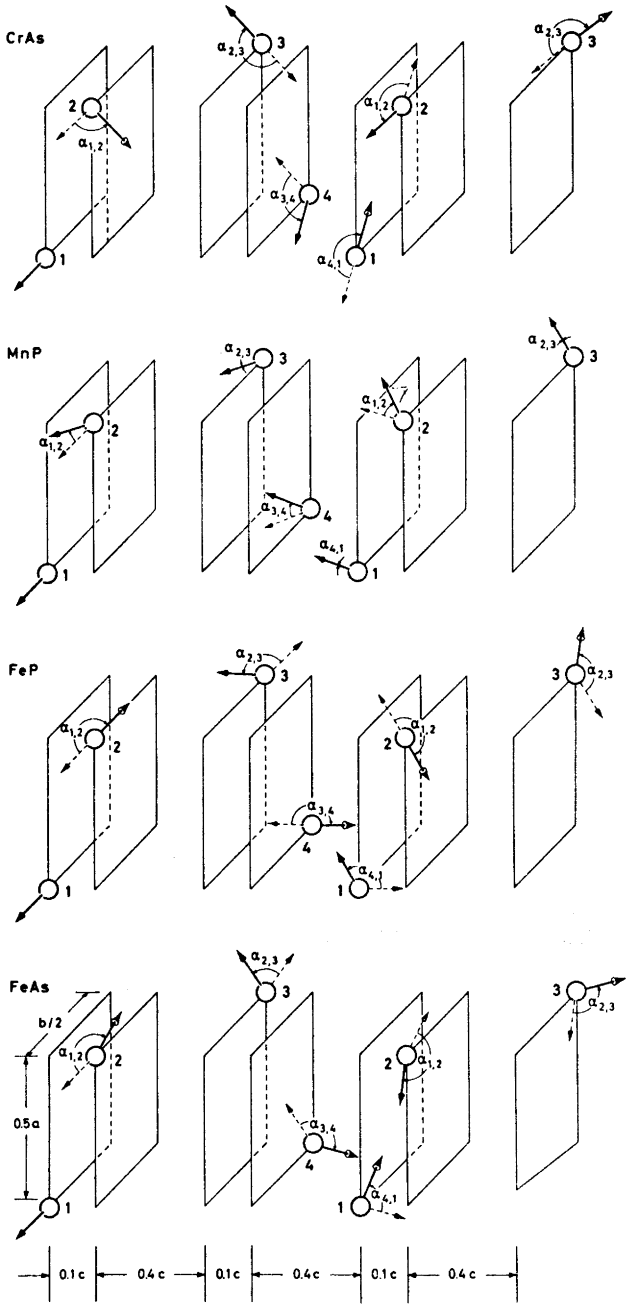

Fig. 5. Spin orientations in the helimagnetic structures of CrAs, MnP, FeP, and FeAs. The numerical values of the indicated angles are:

CrAs:	$\alpha_{1,2}=\alpha_{3,4}=-121°$;	$\alpha_{2,3}=\alpha_{4,1}=+184°$
MnP:	$\alpha_{1,2}=\alpha_{3,4}=+20°$;	$\alpha_{2,3}=\alpha_{4,1}=0°$
FeP:	$\alpha_{1,2}=\alpha_{3,4}=+176°$;	$\alpha_{2,3}=\alpha_{4,1}=-140°$
FeAs:	$\alpha_{1,2}=\alpha_{3,4}=+154°$;	$\alpha_{2,3}=\alpha_{4,1}=-86°$

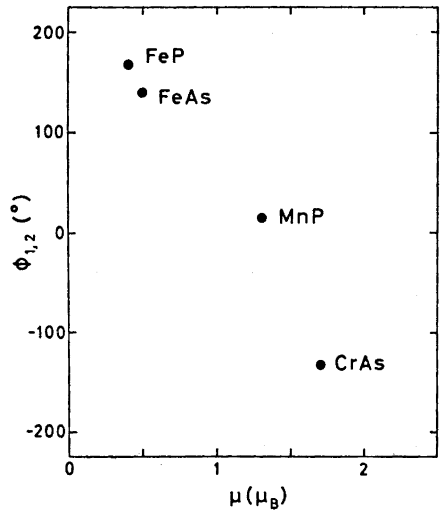

Fig. 6. Magnetic moment *versus* phase angle between independent spirals in CrAs, MnP, FeP, and FeAs. (See also Table 4.)

expected to show consistent helimagnetic properties. The correlations also place in perspective the transition at 50 K of MnP from a helimagnetic state with $\phi_{1,2} \approx 0°$ to a ferromagnetic state in which the condition of collinear spins implies $\phi_{1,2} \equiv 0°$.[2,3,12,13] The self-consistency of these data may also throw light on the absence of cooperative magnetism in MnAs in the temperature range 316 and 393 K where it adopts the MnP type structure.[10,11]

On considering CrAs and MnP, the simplicity of the antiparallel and parallel spin relationships, respectively, between the atoms 2 and 3 (and equivalently on atoms 4 and 1, see Fig. 5) led the present authors [7] to an assumption of a single dominant direct exchange interaction between these atoms. This conception was extended by Boller and Kallel,[8] who discussed the transition between the paramagnetic and helimagnetic states in CrAs in terms of the variation in the interatomic distance between atoms 2 and 3 in relation to the critical value 3.18 Å of the Cr–Cr distance proposed by Goodenough.[26] Although this interpretation appeared to be satisfactory in view of the data provided by Boller and Kallel (see Table 5), it must be rejected on the basis of the corresponding independent data given for CrAs by the present authors.[7] In fact, examination of the shortest metal-metal distances shown in Table 5 for this class of compounds, leads one to conclude that there is no general correlation of the kind envisaged by Boller and Kallel.

The data on the helimagnetic states of FeP and FeAs depart from the simple patterns found in CrAs and MnP (*cf.* Fig. 5). Hence, the angular difference between the moments on atoms 2 and 3 ($\alpha_{2,3}$) is $-140°$ for FeP and $-86°$ for FeAs. This complexity indicates the presence of various competing exchange interactions between atoms 2 and 3. The total number of isotropic exchange parameters operative in this class of compounds may be as high as seven, as proposed by Takeuchi and Motizuki [4] for MnP. A similar total

Table 5. The shortest interatomic metal-metal distances in some compounds with the MnP type crystal structure. For numbering of the atoms see text. Values for critical metal-metal separations are quoted from Goodenough.[26]

Compound	T(K)	Me_1-Me_2 (Å)	Me_2-Me_3 (Å)	Me_1-Me_1 (Å)	Critical Me–Me (Å)	Ref.
VAs	293	2.9_3	3.0_4	3.33	3.21	23
CrP	293	2.768(3)	2.796(3)	3.113(1)	3.18	24
CrAs	80	2.849(3)	3.064(8)	3.575(1)	3.18	7
CrAs	293	2.892(3)	3.030(9)	3.463(1)	3.18	7
CrAs	90	2.836(2)	3.143(21)	3.573	3.18	8
CrAs	285	2.889(3)	3.010(10)	3.445	3.18	8
MnP	293	2.704(3)	2.816(3)	3.172(1)	3.15	24
MnAs	328	2.881(19)	3.387(19)	3.676	3.15	25
FeP	293	2.658(3)	2.791(3)	3.099(1)	3.12	24
FeAs	12	2.795(2)	2.923(5)	3.325(1)	3.12	
FeAs	293	2.789(2)	2.937(5)	3.373(1)	3.12	
CoP	293	2.605(3)	2.751(3)	3.281(1)	3.03	24
CoAs	293	2.708(2)	2.925(5)	3.489(1)	3.03	20

number of parameters were introduced by Bertaut [5] in the form of two isotropic (scalars) and one antisymmetric (tensor) exchange couplings.

The values of the magnetic moments are indicative of low-spin conditions in the cooperative states of CrAs, MnP, FeP, and FeAs (*cf.* Table 4). In particular, the number of unpaired electrons per Fe atom in FeAs appears to increase from 0.5 ± 0.1 to 2.2 ± 0.4 on passing from the helimagnetic to the paramagnetic state. This may be viewed as resulting from a thermal redistribution of electrons between different states, and can account, at least in principle, for the anomalous $\chi^{-1}(T)$ curve in the interval 77 to ~ 300 K.

REFERENCES

1. Kjekshus, A. and Pearson, W. B. *Progr. Solid State Chem.* **1** (1964) 83.
2. Felcher, G. P. *J. Appl. Phys.* **37** (1966) 1056.
3. Forsyth, J. B., Pickart, S. J. and Brown, P. J. *Proc. Phys. Soc.* **88** (1966) 333.
4. Takeuchi, S. and Motizuki, K. *J. Phys. Soc. Japan* **24** (1967) 742.
5. Bertaut, E. F. *J. Appl. Phys.* **40** (1969) 1592.
6. Watanabe, H., Kazama, N., Yamaguchi, Y. and Ohashi, M. *J. Appl. Phys.* **40** (1969) 1128; Kazama, N. and Watanabe, H. *J. Phys. Soc. Japan* **30** (1971) 1319.
7. Selte, K., Kjekshus, A., Jamison, W. E., Andresen, A. F. and Engebretsen, J. E. *Acta Chem. Scand.* **25** (1971) 1703.
8. Boller, H. and Kallel, A. *Solid State Commun.* **9** (1971) 1699.
9. Felcher, G. P., Smith, F. A., Bellavance, D. and Wold, A. *Phys. Rev.* **B 3** (1971) 3046.
10. Menyuk, N., Kafalas, J. A., Dwight, K. and Goodenough, J. B. *Phys. Rev.* **177** (1969) 942.
11. Bacon, G. E. and Street, R. *Nature* **175** (1955) 518.
12. Huber, E. E. and Ridgley, D. H. *J. Appl. Phys.* **34** (1963) 1099.
13. Huber, E. E. and Ridgley, D. H. *Phys. Rev.* **A 135** (1964) 1033.
14. Selte, K. and Kjekshus, A. *Acta Chem. Scand.* **23** (1969) 2047.
15. The Neutron Diffraction Commission, *Acta Cryst.* **A 25** (1969) 391.
16. Watson, R. E. and Freeman, A. J. *Acta Cryst.* **14** (1961) 27.

17. Rietveld, H. M. *J. Appl. Cryst.* **2** (1969) 65.
18. Nelson, J. B. and Riley, D. P. *Proc. Phys. Soc.* **57** (1945) 160.
19. Holseth, H. and Kjekshus, A. *Acta Chem. Scand.* **23** (1969) 3043.
20. Selte, K. and Kjekshus, A. *Acta Chem. Scand.* **25** (1971) 3277.
21. Hansen, M. (and Anderko, K.) *Constitution of Binary Alloys*, McGraw, New York – Toronto – London 1958, p. 163.
22. Heyding, R. D. and Calvert, L. D. *Can. J. Chem.* **35** (1957) 449.
23. Bachmayer, K. and Nowotny, H. *Monatsh.* **86** (1955) 741.
24. Rundqvist, S. and Nawapong, P. C. *Acta Chem. Scand.* **19** (1965) 1006.
25. Wilson, R. H. and Kasper, J. S. *Acta Cryst.* **17** (1964) 95.
26. Goodenough, J. B. *Technical Report No. 345*, Lincoln Laboratory, MIT 1964.

Received December 23, 1971.